Optica Applicata, Vol. XXXIX, No. 2, 2009

An image fusion algorithm based on polyharmonic local sine transform (PHLST)

LIU SHANGZHENG[1], HAN JIUQIANG[1], BOWEN LIU[2], ZHANG XINMAN[1*]

[1]School of Electronic and Information Engineering, Xi'an Jiaotong University, Xi'an, 710049, China

[2]Business Intelligence Lab, University of Science and Technology of China (USTC), Hefei, 230026, China

[*]Corresponding author: ccp9999@sina.com

In this paper, we propose a novel image fusion algorithm based on polyharmonic local sine transform (PHLST). First, we apply PHLST to source image to decompose it into two components: polynomial *p* and residual *r*. Using the Laplace/Possion equation solver, we obtain polynomial *p*. Subtracting *p* from original image, we acquire *r*. In order to reduce noise, *r* is filtered in frequency domain. Next, we fuse *p* and *r* separately. Then we add the composite *p* and composite *r* directly to obtain the fused image. Experiments demonstrate outstanding performance of the method proposed.

Keywords: image fusion, performance metric, polyharmonic local sine transform (PHLST).

1. Introduction

The objective of image fusion is to integrate complementary information from multiple sources of the same scene so that the composite image is more suitable for human visual and machine perception or further image-processing tasks. With the availability of multiple image sources in many fields such as remote sensing, medical imaging, machine vision, and military applications, image fusion has emerged as a new and promising research area. Much effort has been devoted to image fusion techniques in recent years.

A set of two or more source images is obtained of a given scene viewed with different sensors or under different imaging conditions. These source images may have complementary information. How to merge this complementary information into a single image without losing vital information and introducing false information is the core of image fusion. A number of algorithms based on multiscale analysis have been proposed [1–5]. However, these methods were unsatisfactory. The brute-force periodization will cause mismatch when we deal with non-periodic signals. This will lead to the Gibbs phenomenon [6]. Wavelets and wavelet packets essentially use brute-

-force periodization so that it again creates the discontinuity at the end points, and this produces large wavelet/wavelet packet coefficients. The large coefficients will introduce false information in the composite image. And the wavelets are not efficient for textured images [6]. In this study, we suggest a fusion algorithm based on polyharmonic local sine transform (PHLST). PHLST decomposes each source image into two components: the "base" p and the "texture" r of original image. Next, we merge p's and r's, respectively, and obtain composite p and composite r. Then, we add p and r directly to obtain fused image. The algorithm proposed does not introduce the brute-force periodization so that it avoids the disadvantages of algorithms based on wavelet/wavelet packets.

The paper is organized as follows. In Section 2, we give a brief discussion of PHLST and a brief review of Laplace/Possion equation solver proposed by Averbuch, Braverman, and Vozovoi. Section 3 presents the image fusion scheme. In our approach, we apply different fusion rules for p and r, respectively. Preliminary results of the fusion method proposed are presented and discussed in Section 4, and the paper is concluded in Section 5.

2. Polyharmonic local sine transform

The PHLST was first introduced as a model for image compression. We will briefly explain polyharmonic local sine transform. A more detailed description of polyharmonic local transform may be found in [6].

Assume $I(x, y)$ is a spatial-domain image. The main idea of PHLST is that an image $I(x, y)$ can be divided into two parts: p which we call the polyharmonic component of $I(x, y)$ and r which we call the residual of $I(x, y)$. P is a polynomial. R is a geometric series. P represents "base" or "trend" or "predictable" part of the original image, whereas r stands for "texture" or "fluctuation" or "unpredictable" part of the original image. This method coincides with the characteristic of human visual system. Human beings first focus on the noticeable parts of an image. The noticeable parts are the fluctuation of an image. So, we extract texture which is in favor for subsequent manipulation.

$I(x, y)$ is an rectangular image. Let I_{inter} be the interior of $I(x, y)$, I_{bou} be the boundary of $I(x, y)$. For simplicity, $0 \le x \le 1$, $0 \le y \le 1$. By solving polyharmonic equation (1) with given boundary conditions (2), we can obtain the polyharmonic component

$$\Delta^n p = 0 \quad \text{in } I_{\text{inter}}, \quad n = 1, 2, \ldots \tag{1}$$

$$\frac{\partial^{k_l} I}{\partial n^{k_l}} = \frac{\partial^{k_l} p}{\partial n^{k_l}} \quad \text{on } I_{\text{bou}}, \quad l = 0, \ldots, m-1 \tag{2}$$

where $k_l = 2l$, the even order normal derivatives. We need not to consider the odd order normal derivatives because this is automatically guaranteed [6]. The $k_0 = 0$, which

means that $p = f(x, y)$ on the boundary. These boundary values and normal derivatives ensure the function values and the normal derivatives of orders $k_1, \ldots, k_{n-1}$ of p along the boundary to match those of the original image $I(x, y)$ over there.

For $n = 1$, we obtain the following Laplace equation with the Dirichlet boundary condition:

$$\begin{cases} \Delta p = 0 & \text{in} \quad I_{\text{inter}} \\ p = I(x, y) & \text{on} \quad I_{\text{bou}} \end{cases} \tag{3}$$

For $n = 2$, Eq. (1) becomes biharmonic equation with the mixed boundary condition:

$$\begin{cases} \Delta^2 p = 0 & \text{in} \quad I_{\text{inter}} \\ p = I(x, y), \quad \dfrac{\partial^2 p}{\partial n^2} = \dfrac{\partial^2 I}{\partial n^2} & \text{on} \quad I_{\text{bou}} \end{cases} \tag{4}$$

We use the Laplace/Possion equation solver proposed by AVERBUCH *et al*. [7, 8] to solve Eqs. (3) and (4). The ABIV method provides more accurate solutions than those based on the finite difference (FD).

There are several versions of the ABIV method. We choose the simplest and most practical one to solve (3) that does not need to estimate any derivative. It follows the recipe

$$\begin{aligned} p(x, y) = p_1(x, y) + \sum_{k \geq 1} \Big\{ & p2_k^{(1)} g_k(x, 1 - y) + p2_k^{(2)} g_k(y, 1 - x) + \\ & + p2_k^{(3)} g_k(x, y) + p2_k^{(4)} g_k(y, x) \Big\} \end{aligned} \tag{5}$$

where $p_1(x, y)$ is a harmonic polynomial that matches $I(x, y)$ at the four corner points of the image. And its simplest form is:

$$p_1(x, y) = a_3 xy + a_2 x + a_1 y + a_0 \tag{6}$$

Let $p_1(0, 0) = I(0, 0), p_1(0, 1) = I(0, 1), p_1(1, 0) = I(1, 0), p_1(1, 1) = I(1, 1)$, we have

$$\begin{cases} I(0, 0) = a_0 \\ I(0, 1) = a_1 + a_0 \\ I(1, 0) = a_2 + a_0 \\ I(1, 1) = a_3 + a_2 + a_1 + a_0 \end{cases} \tag{7}$$

By solving (7), we can easily obtain the parameters a_i. The function $g_k(x, y)$ is defined as follows:

$$g_k(x, y) = \sin(\pi kx) \frac{\sinh(\pi ky)}{\sinh(\pi k)} \tag{8}$$

and $p_2k(i)$, $i = 1, 2, 3, 4$, are the k-th 1D Fourier sine coefficients of boundary functions $I(x, 0) - p_1(x, 0)$, $I(0, y) - p_1(0, y)$, $I(x, 1) - p_1(x, 1)$, and $I(1, y) - p_1(1, y)$, respectively, where $0 \le x \le 1$, $0 \le y \le 1$. Subtracting $p(x, y)$ from $I(x, y)$, we obtain $r(x, y)$. It can be written as:

$$r(x, y) = \sum_{i \ge 1} \sum_{j \ge 1} s_{ij} \sin(i\pi x) \sin(j\pi y) \tag{9}$$

where s_{ij} is the 2D Fourier sine coefficients of $r(x, y)$.

For a more precise approximation of $I(x, y)$, we can segment an image $I(x, y)$ into a set of rectangular blocks (of different sizes possible) using the characteristic function. There is no overlap between adjacent patches, but adjacent patches may share the boundaries. Then, we decompose each patch into two components: the polyharmonic component p and the residual r, according to the foregoing method.

3. The image fusion scheme

Figure 1 shows a schematic diagram of the basic structure of the image fusion scheme proposed. For simplicity, we make an assumption that there are just two source images, I_1 and I_2, and the fused image is F. We note that all the methods described in this paper can also be extended to cases with more than two source images. An important preprocessing step in image fusion is image registration. Image registration ensures

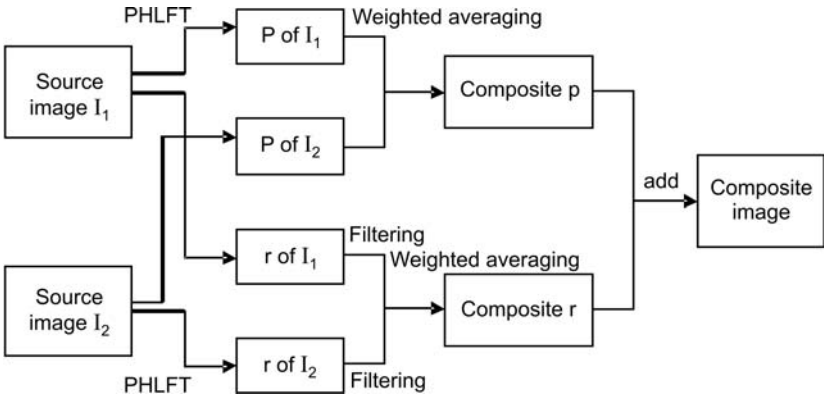

Fig. 1. Block diagram of the algorithm proposed.

that the information from each sensor is referred to the same physical structures in the environment. In this study, we assume that the images to be combined are already perfectly registered.

3.1. Fusion rules

The objective of image fusion is to combine multiple source images of the same scene and obtain a better quality image. The straightforward approach to image fusion is to compute the pixel by pixel average of the input images. Although image averaging is a simple method, a major drawback is that it can cause a decreased image contrast. To avoid a loss of detail, the basic strategy here is to fuse p and r separately to construct a fused PHLST representation from the PHLST representations of the original data.

P represents "base" of the original image. We use the simplest method to compute p averaging.

R represents the "detail" or "texture" of the source image. The larger values in r correspond to the sharper brightness changes and thus to the salient features in the image, such as edges, lines, and region boundaries. Therefore, a good integration rule is to conserve r of the two source images at each point. So, we compute the composite r by the following equation

$$r_F = (r_{I1} + r_{I2})\omega \tag{10}$$

where r_{I1} and r_{I2} represent r's, from I_1 and I_2, respectively, r_F is the composite r.

Subsequently, a composite image is constructed by performing an inverse PHLST. Since the PHLST provides spatial localization, the effect of the direct summing fusion rule can be illustrated in the following two aspects. If the same object appears more distinctly (in other words, with better contrast) in image I_1 than in image I_2, after fusion the object in image I_1 and in image I_2 will be preserved with better contrast than in I_2; in a different scenario, suppose an object appears in the image I_1, while being absent in image I_2, after fusion the object in image I_1 will be preserved and the contrast of the composite image will be enhanced.

3.2. Performance measures

Performance measures are essential to determine the possible benefits of fusion as well as to compare results. Evaluation is usually performed through robust yet impractical subjective trials [9, 10], which is time consuming. Computational objective fusion metrics are an efficient alternative as they need no display equipment or complex organization of an audience. Recent proliferation of image fusion algorithms has prompted the development of reliable and objective ways of evaluating and comparing their performance for any given application [11–15]. Four metrics are considered in this study, which do not require ground truth images. These are: *i*) entropy to evaluate the information contained in the fused image; *ii*) Q_p as defined by PETROVIĆ and

XYDEAS [12], we use the same parameter as well; *iii*) mutual information (MI) proposed by QU *et al.* [14, 16]; *iv*) Q_M, Q_D proposed by HAO CHEN and VARSHNEY [17].

4. Experimental results

In this section, we verify the significant performance of the image fusion method proposed by comparing it with three different image fusion methods using four image fusion metrics. The first algorithm is a Laplace pyramid fusion algorithm [18, 19], where the input images are decomposed using a Laplace pyramid decomposition and the fused image is reconstructed by averaging the low resolution components and selecting the coefficients with the largest amplitude for the high resolution coefficients. The second fusion algorithm used in this study is a shift invariant wavelet fusion algorithm [2], where the source images are decomposed using Harr wavelet filter, the coefficients of the integrated image are computed by choosing the corresponding

T a b l e 1. The fused image measurements of medical images.

	Q_D	Q_M	E	MI	Q_p
Laplace	60.718	40.059	4.2826	1.9259	0.5551
Wavelet	60.605	39.847	4.2421	2.0208	0.5371
NSCT	62.73	41.127	4.3049	1.8243	0.5289
PHLST	56.114	36.87	4.4495	3.5708	0.5919

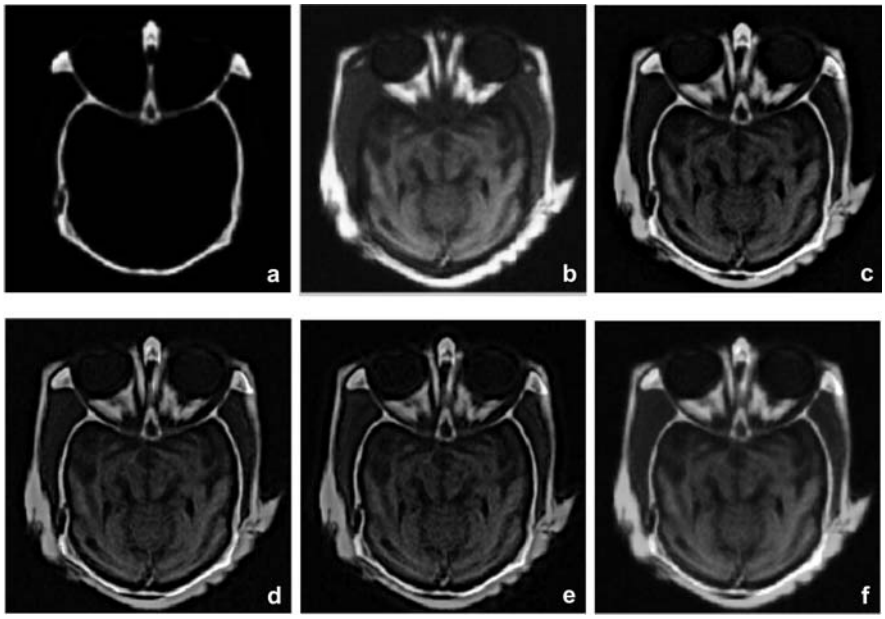

Fig. 2. Testing image set 1: medical images.

coefficients of input images with the largest amplitude in high frequency bands and by averaging the coefficients of base band. The third fusion algorithm is a non--subsampled contourlet fusion (NSCT) algorithm [20, 21], the fusion rule is the same as the one in wavelet fusion algorithm. The number of decomposition levels is three in all the methods.

4.1. Experimental results of medical imagery CT and MRI

In Figures 2–4: **a** and **b** are the input images, **c** is the fused image using Laplace method, **d** is the fused image using shift invariant wavelet method, **e** is the fused image using NSCT method, **f** is the fused image using PHLST method. The quantitative assessments of fused images are listed in Tab. 1. From this table, we can see that the performance of the algorithm proposed is best according to all metrics. The fused images are illustrated in Figs. 2**c**–2**f**.

4.2. Experimental results of visible and IR images

The image quality evaluation results of the fused images by the four methods are given in Tab. 2. The fused images are shown in Figs. 3**c**–3**f**. The performance of

T a b l e 2. The fused image measurements of visible and IR image.

	Q_D	Q_M	E	MI	Q_p
Laplace	33.7695	56.6074	4.5548	1.0301	0.6211
Wavelet	31.8273	56.6074	4.4736	1.037	0.6162
NSCT	30.9515	51.8811	4.4189	1.04	0.6110
PHLST	31.1143	52.1593	4.7058	1.1759	0.6561

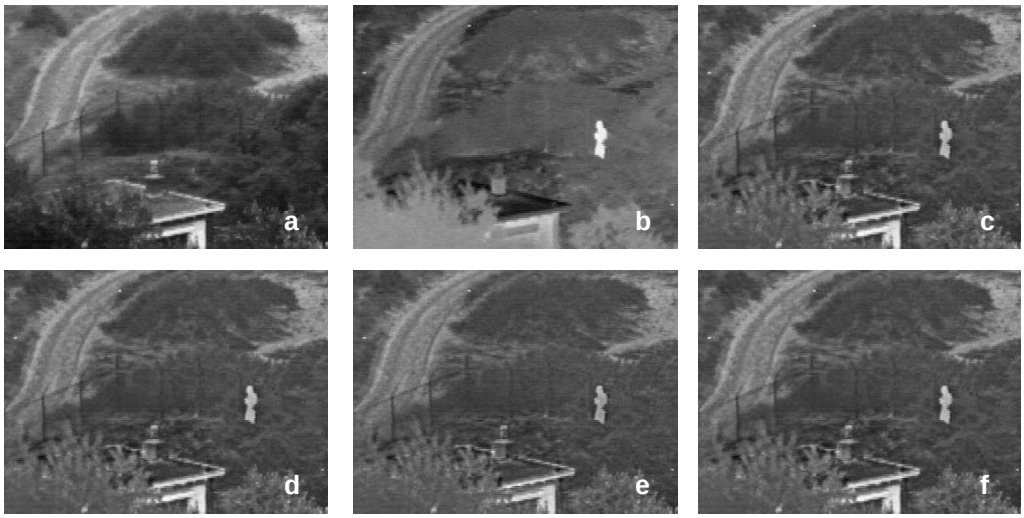

Fig. 3. Testing image set 2: visible and IR image.

the algorithm proposed is best according to metric E, MI, and Q_p. Judging by Q_D and Q_M, the best method is NSCT. PHLST ranks as the second, but the differences of the two methods are very small, with only (31.1143 – 30.9515)/30.9515 = 0.53%, (52.1593 – 51.8811)/51.8811 = 0.54%.

4.3. Experimental results of SAR images

The quantitative assessments of fused images are listed in Tab. 3. The fused images are given by Figs. 4**c**–4**f**. The performance of the algorithm proposed is best according to metrics E, MI, and Q_D, Q_M. Judging by Q_p, the performance of the algorithm proposed ranks as the third, but the difference of the first and the third is very small, with only (0.8806 – 0.8723)/1=0.83%. Notice that through visual inspection, it is fairly difficult to discriminate between the four fused images.

T a b l e 3. The fused image measurements of remote sensing images.

	Q_D	Q_M	E	MI	Q_p
Laplace	112.22	74.213	5.0881	1.8127	0.8704
Wavelet	104.27	68.912	5.0193	1.8818	0.8784
NSCT	99.199	65.668	5.0171	1.8780	0.8806
PHLST	95.915	63.457	5.1377	1.9006	0.8723

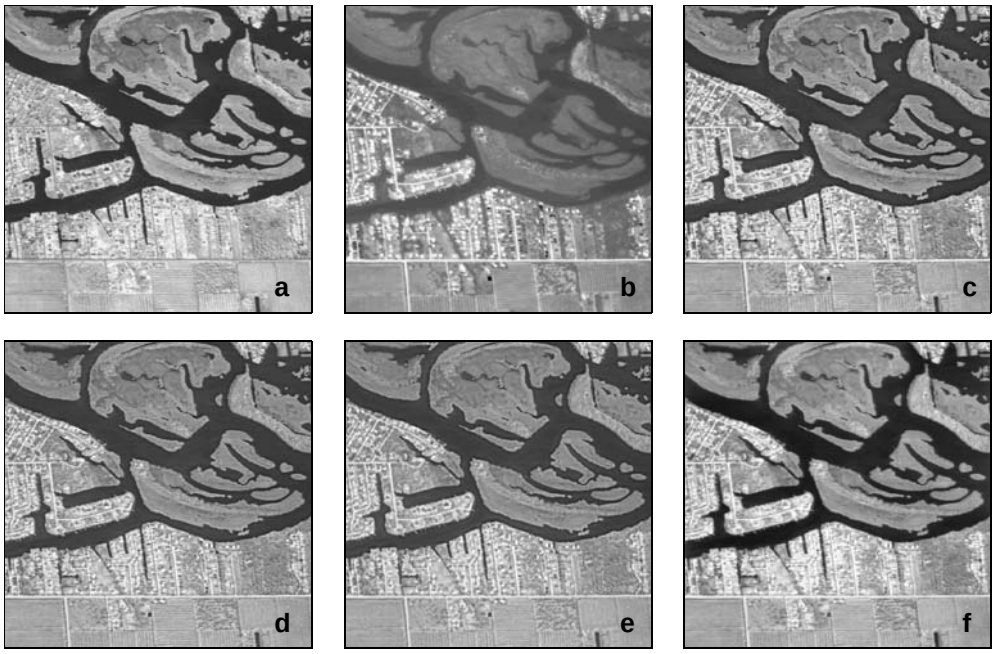

Fig. 4. Testing image set 3: SAR images.

5. Conclusions

We have presented in this paper a new approach to multisensor image pixel data fusion using PHLST. We demonstrate image fusion using images with different scene information from the different types of sensor. These examples show that the image fusion method is capable of extracting the important information from the source images and placing it in the fused image. Experimental results demonstrate the significant performance of the algorithm proposed.

Acknowledgements – This work has been supported by the National Natural Science Foundation of China under Project 60602025. The original CT and MRI images were kindly supplied by Dr. Oliver Rockinger, the visible and IR images by Alexander Toet of the TNO Human Factors Research Institute, the remote sensing images by Dr. Vladimir Petrovic of Manchester University. The wavelet and Laplace fusion codes are from The Image Fusion Toolbox for Matlab developed by Oliver Rockinger, Metapix, the nonsubsampled contourlet fusion code is from Nonsubsampled Contourlet Toolbox provided by Jianping Zhou *et al*. These images and codes are available online at www.imagefusion.org.

References

[1] ZHANG X., HAN J., *Multiscale contrast image fusion scheme with performance measures*, Optica Applicata **34**(3), 2004, pp. 453–461.

[2] ROCKINGER O., *Pixel-level fusion of image sequence using wavelet frames*, Proceedings of the 16th Leeds Applied Shape Research Workshop, Leeds University Press, 1996.

[3] THAM J.Y., SHEN L., LEE S.L., TAN H.H., *General approach for analysis and application of discrete multiwavelet transforms*, IEEE Transactions on Signal Processing **48**(2), 2000, pp. 457–464.

[4] WANG H., PENG J., WU W., *Fusion algorithm for multisensor images based on discrete multiwavelet transform*, IEE Proceedings: Vision, Image and Signal Processing **149**(5), 2002, pp. 283–289.

[5] IOANNIDOU S., KARATHANASSI V., *Investigation of the dual-tree complex and shift-invariant discrete wavelet transforms on quickbird image fusion*, IEEE Geoscience and Remote Sensing Letters **4**(1), 2007, pp. 166–170.

[6] SAITO N., REMY J.-F., *The polyharmonic local sine transform: A new tool for local image analysis and synthesis without edge effect*, Applied and Computational Harmonic Analysis **20**(1), 2006, pp. 41–73.

[7] AVERBUCH A., ISRAELI M., VOZOVOI L., *A fast Poisson solver of arbitrary order accuracy in rectangular regions*, SIAM Journal on Scientific Computing **19**(3), 1998, pp. 933–952.

[8] BRAVERMAN E., ISRAELI M., AVERBUCH A., VOZOVOI L., *A fast 3D Poisson solver of arbitrary order accuracy*, Journal of Computational Physics **144**(1), 1998, pp. 109–136.

[9] TOET A., FRANKEN E.M., *Perceptual evaluation of different image fusion schemes*, Displays **24**(1), 2003, pp. 25–37.

[10] PETROVIĆ V., *Subjective tests for image fusion evaluation and objective metric validation*, Information Fusion **8**(2), 2007, pp. 208–216.

[11] PETROVIĆ V., XYDEAS C., *Objective evaluation of signal-level image fusion performance*, Optical Engineering **44**(8), 2005.

[12] PETROVIĆ V., XYDEAS C., *Sensor noise effects on signal-level image fusion performance*, Information Fusion **4**(3), 2003, pp. 167–183.

[13] PIELLA G., HEIJMANS H., *A new quality metric for image fusion*, IEEE International Conference on Image Processing, Vol. 3, 2003, pp. 173–176.

[14] QU G., ZHANG D., YAN P., *Information measure for performance of image fusion*, Electronics Letters **38**(7), 2002, pp. 313–315.
[15] YIN CHEN, BLUM R.S., *A new automated quality assessment algorithm for night vision image fusion*, Proceedings of CISS'07, 41-st Annual Conference on Information Science and Systems, March 14–16, 2007, pp. 518–523.
[16] COLE-RHODES A.A., JOHNSON K.L., LEMOIGNE J., ZAVORIN I., *Multiresolution registration of remote sensing imagery by optimization of mutual information using a stochastic gradient*, IEEE Transaction on Image Processing **12**(12), 2003, pp. 1495–1511.
[17] HAO CHEN, VARSHNEY P.K., *A human perception inspired quality metric for image fusion based on regional information*, Information Fusion **8**(2), 2007, pp. 193–207.
[18] BURT P.J., *The pyramid as structure for efficient computation*, [In] *Multiresolution Image Processing and Analysis*, [Ed.] A. Rosenfeld, Springer-Verlag, New York, Berlin, 1984, pp. 6–35.
[19] BURT P.J., ADELSON E.H., *Merging images through pattern decomposition*, Proceedings of SPIE **575**, 1985, pp. 173–181.
[20] JIANPING ZHOU, CUNHA A.L., MINH N. DO, *Nonsubsampled contourlet transform: construction and application in enhancement*, IEEE International Conference on Image Processing 2005, Vol. 1, 2005, pp. 469–472.
[21] CUNHA A.L., JIANPING ZHOU, MINH N. DO, *The nonsubsampled contourlet transform: Theory, design, and applications*, IEEE Transactions on Image Processing **15**(10), 2006, pp. 3089–3101.

Received April 10, 2008